Modeling Earth Systems and Environment (2019) 5:1627–1633
https://doi.org/10.1007/s40808-019-00612-z

ORIGINAL ARTICLE

Graphene oxide–tannic acid nanocomposite as an efficient adsorbent for the removal of malachite green from water samples

Alaa Al-Kinani[1] · Mohammad Gheibi[2] · Mohammad Eftekhari[3]

Received: 2 March 2019 / Accepted: 3 June 2019 / Published online: 6 June 2019

Abstract

Graphene oxide–tannic acid (GO–TA) nanocomposite was used as an efficient, green and rapid adsorbent for the removal of malachite green (MG) from water samples. GO was synthesized from graphite by Hummer method and modified by tannic acid to produce GO–TA nanocomposite. The results of Fourier Transform-Infrared Spectroscopy, atomic force microscopy and Brunner–Emmett–Teller show that the GO–TA nanocomposite with the surface area of 79.6 $m^2\ g^{-1}$ has been synthesized successfully. The effect of pH, removal time, initial concentration of MG and stirring rate on adsorption capacity of MG were investigated and the experimental isotherm data were analyzed using the Langmuir and Freundlich equations. Also, two kinetic models including the pseudo first- and second-order equations were investigated and kinetic parameters were calculated and discussed. The results show that, the adsorption of MG onto the GO–TA nanocomposite followed by both Langmuir and Freundlich isotherms with a maximum theoretical adsorption capacity of 500 mg g^{-1} at 25 °C. Also, the results of kinetic models show that the adsorption of MG onto the GO–TA nanocomposite could be described by the pseudo first order kinetic model. Finally, based on the obtained results, it was concluded that GO–TA nanocomposite is very efficient and rapid adsorbent for the removal of MG from water samples.

Keywords Graphene oxide–tannic acid nanocomposite · Malachite green · Kinetic models · Adsorption isotherm · Removal · Adsorption

Introduction

The process of extending the industrialization in developing countries has considerably increased the emission of various contaminants in soil, air and aquatic environments. In the near future, countries must pay significant costs to compensate for the damages resulting from such technological and industrial advances (Reife et al. 1996). Regarding dye contaminations, the presence of malachite green (MG) in the wastewater of industrial activities could be pointed out as one of these contaminants. MG as a dye compound with a tri-phenylmethane chemical structure, has been widely used to deal with ectoparasites, fungi and bacteria in fish and crustaceans breeding (Andersen et al. 2006). Furthermore, this green substance is also used in various industries for dying different materials such as silk, wool, hemp, leather and papers (Gessner and Mayer 2000). While MG could control infections resulting from bacteria, fungi, protozoa, cestode, nematode, trematode, and crustaceans in aquaculture, it also involves toxic impacts on human which could lead to the tumor formation and cancer in mammals (Srivastava et al. 2004). Also, by extension of MG into the surface waters, it could be prevent the penetration of light into the depth of water. Therefore, its removal from water or wastewater samples is highly demanded. There are different mechanisms for the removal of MG from water samples including adsorption process (Ghaedi et al. 2014; Sadegh et al. 2015; Dahri et al. 2014; Yu et al. 2012; Santhi et al. 2010; Wang et al. 2015), chemical precipitation (Lee et al. 2013), membrane technology (Xu et al. 2012), photo-oxidation (Rajabi et al. 2013) and biological treatments (Daneshvar et al. 2007). Among the mentioned methods, adsorption mechanism is most popular due to its relatively rapidity, simplicity,

✉ Mohammad Eftekhari
meftekhari85@yahoo.com

[1] General Directorate of Education in Baghdad Governorate, Iraqi Ministry of Education, Baghdad, Iraq

[2] Department of Civil and Environmental Engineering, Ferdowsi University of Mashhad, Mashhad, Iran

[3] Department of Chemistry, Faculty of Sciences, University of Neyshabur, Neyshabur, Iran

wide range of adsorbents and also low cost for operation (Gupta and Suhas 2009; Hameed 2009).

Graphene oxide (GO) is produced by chemically oxidation of graphite followed by ultrasonication of the synthesized graphite oxide. Its impressive features such as high conductivity and surface area, excellent biocompatibility and ability to modify its surface, makes it a good candidate in different research fields (Zhu et al. 2010; Chen et al. 2012). Tannic acid (TA) is a natural polyphenol which possess different hydroxybenzene groups in its structure; and it could be used to modify the surface of GO for interaction with a chemical compounds such as heavy metals or cationic dyes. In the present research work, the efficiency of GO–TA nanocomposite for the removal of MG from water samples is investigated. The effect of main parameters influencing the adsorption capacity of MG including pH, removal time, initial concentration of MG and stirring rate were studied and optimized. Also, kinetic models and adsorption isotherms were investigated and interpreted.

Materials and methods

Reagents

Tannic acid (> 98%) and extra pure graphite powder (≥ 99.5%) were purchased from Merck Company (Germany). Tris-buffer agent was purchased from Sigma Aldrich, USA. Sodium nitrate ($NaNO_3$, Merck, Germany), potassium permanganate ($KMnO_4$, Merck, Germany), H_2SO_4 (98%, Merck, Germany) and H_2O_2 (30% Merck, Germany) were used for oxidation of graphite to graphite oxide. A solution of 1000 mg L^{-1} Malachite Green (MG, Sigma Aldrich, USA) was prepared in deionized water and the working solutions were prepared by appropriate dilution of stock solution.

Instruments

An Agilent spectrophotometer model 8453 equipped with photodiode-array detector was used (the maximum wavelength of MG was 620 nm). The measurement of pH was performed using Metrohm 827 pH meter (Switzerland). A Centrifuge (Andreas Hettich D72, Germany) was used for separation of adsorbent from the sample solution. Atomic Force Microscopy (AFM, Ara Research, Iran) was used to determine the thickness of the synthesized GO–TA nanocomposite. Surface area analysis for GO–TA nanocomposite was carried out using the Brunner–Emmett–Teller (BET) method (Belsorp mini II, Japan) and FT-IR instrument (Thermo Nicolet model AVATAR 370, USA) was used to record of FT-IR spectrum of GO and GO–TA.

Synthesis of GO and GO–TA nanocomposite

GO and GO–TA nanocomposite were synthesized according to our previous research (Eftekhari et al. 2018). Briefly, 23 mL of concentrated H_2SO_4 was added to the 1 g of graphite powder and the resulting mixture was stirred for 30 min at 5 °C. Then, by addition of 0.5 g $NaNO_3$ to the mixture, it was stirred at 15–20 °C for 30 min. Subsequently, 3 g $KMnO_4$ was added to the mixture within 1 h and it was stirred at 15–20 °C for another 90 min followed by heating to 35 °C and stirring for 2 h at this temperature. An aliquot of 100 mL deionized water was poured into the mixture followed by immediately addition of 5 mL H_2O_2 to it. Finally, the resulting graphite oxide was washed with deionized water for several times (to obtain pH 6–7 for supernatant) and ultrasonicated for 1 h to synthesize GO nanosheets. The synthesized GO was centrifuged at 3000 rpm and dried at 55 °C for 12 h.

In order to synthesize TA-GO nanocomposite, a solution of 1 g L^{-1} GO buffered with 0.1 mol L^{-1} Tris buffer at pH 8.5 and ultrasonicated for 30 min. Then, 0.25 g of TA was added to the mixture and stirred for 24 h at room temperature. The resulting mixture was centrifuged at 3000 rpm, washed with deionized water and dried at 50 °C for 12 h.

Removal procedure

To the 25 mL of 50 mg L^{-1} MG at the pH value of 8.0, an amounts of 5 mg GO–TA nanocomposite was added. The resulting mixture was stirred by a magnetic stirrer at 300 rpm for 25 min. Then, by centrifuging of the mixture at 2500 rpm for 10 min, the concentration of the remaining MG was determined by measurement the absorbance of its supernatant at 620 nm. The amount of MG adsorbed on GO–TA nanocomposite (Adsorption capacity, mg g^{-1}) was determined according to the Eq. 1.

$$\text{Adsorption capacity} = \frac{(C_i - C_e)V}{m}, \quad (1)$$

where C_i and C_e are the initial and equilibrium concentration of MG. V is the volume of sample solution in Lit and m is the amounts of GO–TA nanocomposite in g.

Results and discussion

Characterization of adsorbent

The synthesized GO–TA nanocomposite was characterized by FT-IR spectrophotometry, AFM images and BET analysis. The result of FT-IR spectrophotometry was shown in

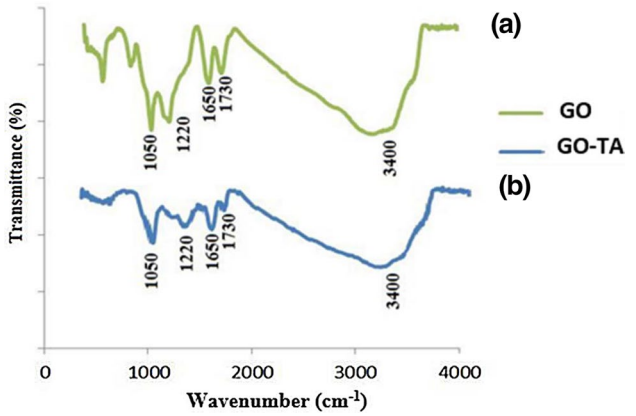

Fig. 1 FT-IR spectrum of GO (a) and TA-GO (b)

Fig. 1. As it could be seen in Fig. 1a, the peaks of OH– group (3400 cm^{-1}), epoxy groups (1220 cm^{-1}), C–O (1050 cm^{-1}), C=O (1730 cm^{-1}) and C=C (1650 cm^{-1}) show that GO was synthesized successfully. However, the spectrum of Fig. 1b (for GO–TA) shows a dramatically decreases at 1220 cm^{-1} due to the nucleophilic SN_2 reaction of the hydroxyl groups of TA with epoxy rings of GO (Eftekhari et al. 2018).

The results of AFM analysis in Fig. 2 show that, the roughness of GO–TA is about 8 nm which significantly higher than the bare GO (about 1.65 nm). Therefore, it could be concluded that the surface of GO changes due to its modification with TA. Finally, BET analysis were performed on GO and GO–TA. As it could be seen in Fig. 3, the obtained surface areas for GO and GO–TA are 54.2 $m^2\ g^{-1}$ and 79.6 $m^2\ g^{-1}$, respectively, which clearly show that the modification of GO with TA occurred successfully.

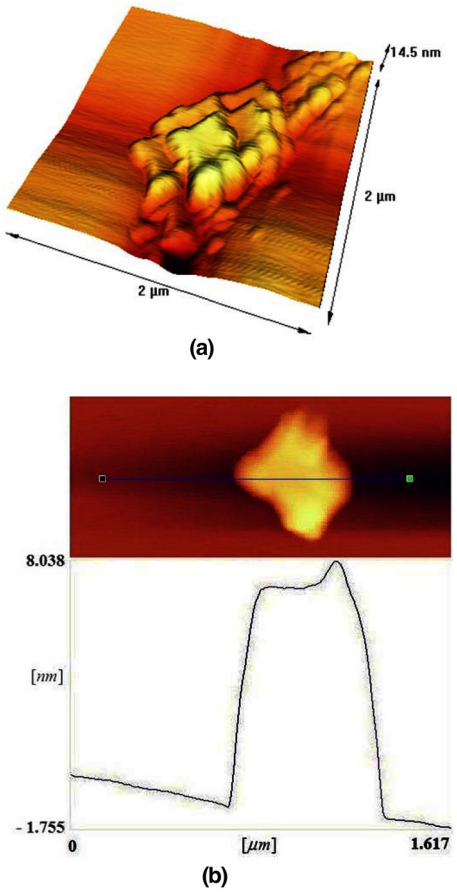

Fig. 2 AFM images of GO–TA (**a**, **b**)

Effect of pH

pH has an important effect on the adsorption capacity of MG by its effect on the surface charge of adsorbent. The influence of pH on the adsorption capacity of MG was studied in the range of 3–9 and demonstrated in Fig. 4. As it can be seen, pH 5–9 for both 50 and 100 mg L^{-1} MG and pH 8–9 for 100 mg L^{-1} MG provide maximum adsorption capacities for MG. In order to explain the effect of pH; zeta potential analyses were performed to determine the surface charge of adsorbent at various pH values. Based on the results, at the pH of 3, 4, 5, 6, 8 and 9; the zeta potential values are +0.34, − 17.5, − 22.2, − 24.2, − 30.3 mv and − 33.6 mv, respectively. Therefore, there are three main mechanisms for the adsorption of MG onto the GO–TA nanocomposite including: (1) Electrostatic interaction between negative charged GO–TA nanocomposite (dissociation of free carboxylic acid groups) and MG, (2) ion dipolar interactions of OH groups on TA and MG and (3) π–π interaction of GO–TA nanocomposite and phenyl groups of MG. Therefore, for further experiments pH 8 was considered as the optimum value.

Effect of removal time and the concentration of MG

The effect of removal time on the adsorption capacity of MG was investigated in the range of 10–75 min and the

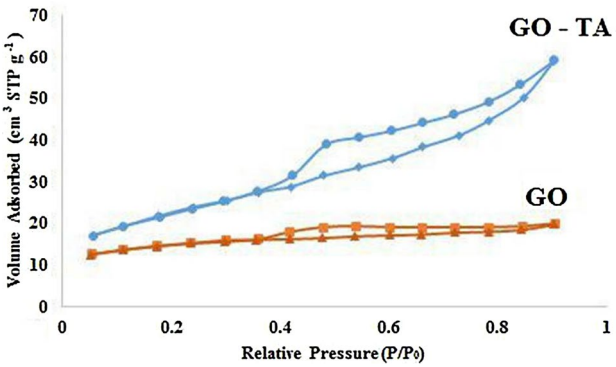

Fig. 3 N_2 adsorption–desorption isotherms for GO and GO–TA

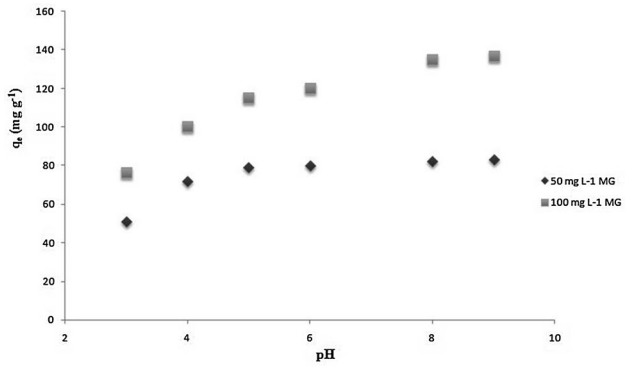

Fig. 4 Effect of pH on the adsorption capacity of MG. Conditions: 50, 100 mg L^{-1} MG, removal time: 25 min, 5 mg GO–TA nanocomposite as adsorbent and 300 rpm stirring rate

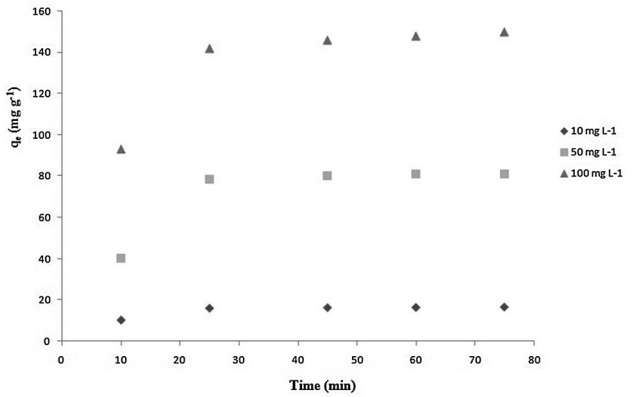

Fig. 5 Effect of removal time on the adsorption capacity of MG. Conditions: 10, 50 and 100 mg L^{-1} MG, pH: 8, 5 mg GO–TA nanocomposite as adsorbent and stirring rate 300 rpm

results are demonstrated in Fig. 5. As the results shown, 25 min removal time is an adequate time to reach the maximum adsorption capacity. Therefore, it was considered as an optimum value. Also, different concentrations of MG in the range of 10–100 mg L^{-1} were tested and based on the results; by increase of the concentration of MG, the adsorption capacity increases which may be due to the higher diffusion rate of MG onto the GO–TA nanocomposite.

Effect of stirring rate

The stirring rate of sample solution was studied in the range of 100–500 rpm and the obtained results are presented in Fig. 6. As it could be seen, the stirring rates higher than 200 rpm have no impressive effect on the adsorption capacities of MG. Therefore, in order to obtain uniform agitation, 300 rpm was selected as the optimum value.

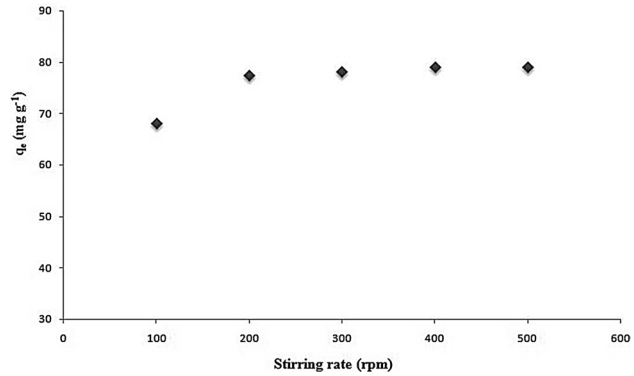

Fig. 6 Effect of stirring rate on the adsorption capacity of MG. Conditions: 50 mg L^{-1} MG, pH: 8, 5 mg GO–TA nanocomposite as adsorbent and 300 rpm stirring rate

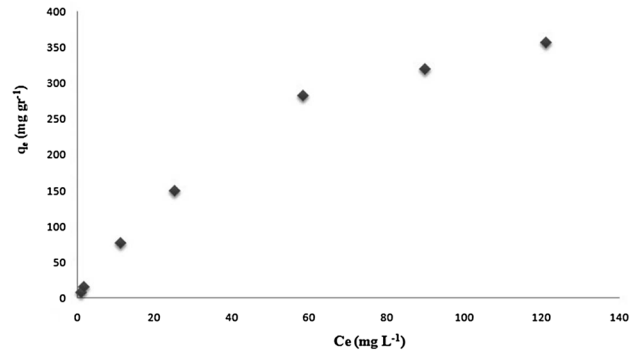

Fig. 7 Plotting of q_e versus C_e for calculating of practical q_{max}. Conditions: 5–300 mg L^{-1} MG, 5 mg amounts of adsorbent, removal time: 45 min

Adsorption study

To study the mechanism of adsorption of MG onto the GO–TA nanocomposite, two isotherms including Langmuir and Freundlich were investigated and discussed.

Langmuir isotherm which is reliable for monolayer adsorption of analyte is expressed in Eq. 2, where q_e is the equilibrium adsorption capacity (mg g^{-1}), C_e is the equilibrium concentration of MG (mg L^{-1}), q_{max} is the theoretical maximum adsorption capacity (mg g^{-1}) and K_{ads} is the constant (Iranzad et al. 2018).

$$C_e/q_e = C_e/q_{max} + K_{ads}/q_{max}. \quad (2)$$

By plotting of C_e/q_e versus C_e, the values of q_{max} and K_{ads} were calculated from the slope and intercept of curve which equal to 500 and 50.8, respectively ($R^2 = 0.98$). Also, the practical q_{max} was determined by depicting of q_e versus C_e (Fig. 7) which is 283.4 mg g^{-1}.

Freundlich equation is another isotherm reliable for the multilayer adsorption of analyte and expressed in Eq. 3.

$$\text{Log } q_e = \log K_F + 1/n \log C_e. \quad (3)$$

K_F is adsorption capacity (mg g^{-1}) and n is the favorability. By depicting of log q_e versus log C_e, these parameters could be calculated from the intercept and slope of the curve, respectively. Based on the Freundlich equation, the values of K_F and n are 1.08 and 1.02, respectively ($R^2 = 0.98$) which show that the adsorption of MG onto the GO–TA nanocomposite is favorable ($n > 1$). Also, the results of R^2 values for the Langmuir and Freundlich equations show that the adsorption of MG onto the GO–TA nanocomposite was governed by both Langmuir and Freundlich equations.

Kinetic study for the adsorption of MG onto the GO–TA nanocomposite

Pseudo-first-order kinetic equation

The linear form of pseudo-first-order model is expressed by Eq. 4 (Akrami et al. 2019):

$$\text{Log}\left(q_e - q_t\right) = \log q_e - \frac{k1}{2.303}t. \quad (4)$$

By depicting of log ($q_e - q_t$) versus t, the values of k_1 (rate constant for the first order kinetic model) and q_e could be obtained from the slope and intercept of the plot, respectively (Fig. 8). The results of k_1, q_e and R^2 for different concentrations of MG are presented in Table 1. As it shown, the R^2 values ($R^2 \geq 0.94$) indicate that the adsorption of MG followed by pseudo-first-order kinetic equation. Also, in pseudo-first-order kinetic system, the calculated q_e (cal) values are very nearby to the experimental results (Table 1) which clearly show that the adsorption kinetic of MG is governed by the pseudo first-order kinetic equation.

Table 1 The first order adsorption rate constants and calculated and experimental q_e values for MG

Dye	Concentration (mg L^{-1})	First order kinetic model			
		q_e (exp)	q_e (cal)	k_1	R^2
Malachite green	10	19.76	21.94	0.10	0.94
	50	80.00	95.48	0.07	0.99
	100	151.80	168.31	0.08	0.96
	200	283.40	331.60	0.10	0.96

Pseudo-second-order kinetic equation

Equations 5 and 6 show the pseudo-second order kinetic equation and its linear form, respectively (Akrami et al. 2019).

$$\frac{dqt}{dt} = k_2\left(q_e - q_t\right)^2, \quad (5)$$

$$\frac{t}{qt} = \frac{1}{K_2 qe^2} + \frac{1}{qe}t. \quad (6)$$

The initial sorption rate, h (mg g^{-1} min^{-1}) is defined as: $h = k_2 q_e^2$.

Figure 9 shows the plot of t/q_t versus t at different concentrations of MG and the values of q_e and h could be obtained from the slope and intercept of the plot, respectively. The results of k_2 (rate constant of the pseudo-second-order kinetic equation in g mg^{-1} min^{-1}), h and R^2 are represented in Table 2. Based on the results, the R^2 values for MG dye are in the range of 0.82–0.92 which lowers than the R^2 values for the pseudo-first-order kinetic equation. Also, in pseudo-second-order kinetic system, the calculated q_e (cal) values are far from the experimental q_e values (see Table 2). Therefore, pseudo second order kinetic equation is not usable for prediction of adsorption data.

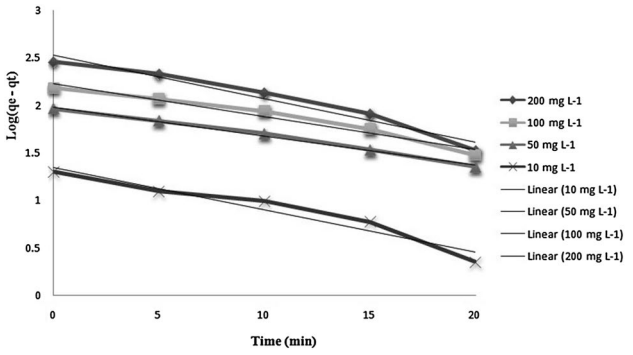

Fig. 8 Pseudo-first-order kinetics for MG adsorption onto GO–TA nanocomposite. Conditions: 10–200 mg L^{-1} concentration of MG, 5 mg amounts of GO–TA nanocomposite as adsorbent

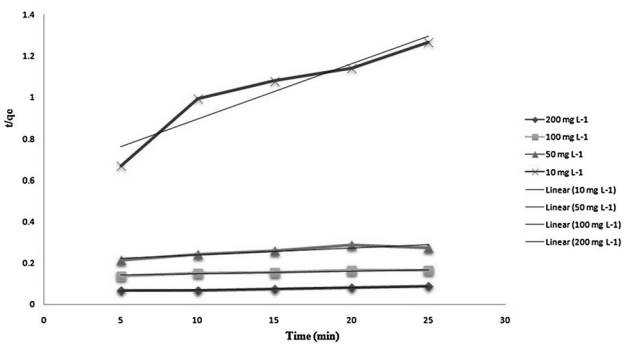

Fig. 9 Pseudo-second-order kinetics for MG adsorption onto GO–TA nanocomposite. Conditions: 10–200 mg L^{-1} concentration of MG, 5 mg amounts of GO–TA nanocomposite as adsorbent

Table 2 The second order adsorption rate constants and calculated and experimental q_e values for different initial MG concentrations

Dye	Concentration (mg L^{-1})	Second order kinetic model				
		q_e (exp)	q_e (cal)	k_2	h	R^2
Malachite green	10	19.76	37.31	0.0011	1.59	0.89
	50	80.00	294.12	0.000056	4.89	0.82
	100	151.80	769.23	0.000012	7.36	0.92
	200	283.40	909.10	0.00002	16.98	0.92

Table 3 Comparison of TA-GO nanocomposite with other adsorbents for the removal of MG

Adsorbent	Theoretical q_{max} (mg g^{-1})	References
Activated carbon from *Ricinus communis*	27.78	Santhi et al. (2010)
β-Cyclodextrin-graphene oxide nanocomposites	740.74	Wang et al. (2015)
Wood apple shell	80.645	Sartape et al. (2017)
Degreased coffee bean	55.3	Baek et al. (2010)
Reduced graphene oxide	462.2	Gupta and Khatri (2017)
Effective microorganisms based compost	150.8	Bhagavathi Pushpa et al. (2015)
Organically modified hydroxyapatite	188.18	El-Zahhar and Awwad (2016)
Tannic acid-graphene oxide nanocomposite	500.0	Present work

Comparison to other adsorbent

The efficiency of the proposed GO–TA nanocomposite was compared by other adsorbents for the removal of MG and presented in Table 3. As it shown, GO–TA nanocomposite has high adsorption capacity and short removal time. Therefore, it could be consider as a powerful and very efficient adsorbent for the removal of MG from different water samples.

Conclusion

Graphene oxide–tannic acid (GO–TA) nanocomposite as an effective and green adsorbent was used for the removal of malachite green from water samples. Graphene oxide was synthesized by Hummer method and modified by tannic acid to produce GO–TA nanocomposite. The synthesized GO–TA nanocomposite was then used as adsorbent for the removal of MG. After optimizing the main parameters affecting the adsorption capacity, two adsorption isotherms including Langmuir and Freundlich were studied and the results show that the adsorption of MG followed by both Langmuir and Freundlich isotherms. Also, by investigation of kinetic models including pseudo first and second order equations, it was revealed that the adsorption of MG governed by pseudo first order kinetic model. The advantages such as availability, high adsorption capacity (500 mg g^{-1} MG), ease of synthesize and short removal time makes GO–TA nanocomposite as an efficient adsorbent for the removal of MG from water samples.

Acknowledgements The authors wish to thanks the University of Neyshabur for their assistance to complete this project (Grant no. 145).

Compliance with ethical standards

Conflict of interest The authors declared that, they have no conflict of interest.

References

Akrami M, Danesh S, Eftekhari M (2019) Comparative study on the removal of cationic dyes using different graphene oxide forms. J Inorg Organomet Polym. https://doi.org/10.1007/s10904-019-01140-0 **(in press)**

Andersen WC, Turnipseed SB, Roybal JE (2006) Quantitative and confirmatory analyses of malachite green and leucomalachite green residues in fish and shrimp. J Agric Food Chem 54:4517–4523

Baek MH, Ijagbemi CO, Se-Jin O, Kim DS (2010) Removal of Malachite Green from aqueous solution using degreased coffee bean. J Hazard Mater 176:820–828

Bhagavathi Pushpa T, Vijayaraghavan J, Sardhar Basha SJ, Sekaran V, Vijayaraghavan K, Jegan J (2015) Investigation on removal of malachite green using EM based compost as adsorbent. Ecotoxicol Environ Saf 118:177–182

Chen D, Feng H, Li J (2012) Graphene oxide: preparation, functionalization, and electrochemical applications. Chem Rev 112:6027–6053

Dahri MK, Rahimi Kooh MR, Lim LBL (2014) Water remediation using low cost adsorbent walnut shell for removal of malachite

green: equilibrium, kinetics, thermodynamic and regeneration studies. J Environ Chem Eng 2:1434–1444
Daneshvar N, Ayazloo M, Khataee AR, Pourhassan M (2007) Biological decolorization of dye solution containing Malachite Green by microalgae *Cosmarium* sp. Bioresour Technol 98:1176–1182
Eftekhari M, Gheibi M, Akrami M, Iranzad F (2018) Solid-phase extraction of ultra-trace levels of lead using tannic acid-coated graphene oxide as an efficient adsorbent followed by electrothermal atomic absorption spectrometry; response surface methodology-central composite design. New J Chem 42:1159–1168
El-Zahhar AA, Awwad NS (2016) Removal of malachite green dye from aqueous solutions using organically modified hydroxyapatite. J Environ Chem Eng 4:633–638
Gessner T, Mayer U (2000) Triarylmethane and diarylmethane dyes, ullmann's encyclopedia of industrial chemistry. Wiley-VCH Verlag GmbH & Co. KGaA, Hoboken
Ghaedi M, Ansari A, Habibi MH, Asghari AR (2014) Removal of malachite green from aqueous solution by zinc oxide nanoparticle loaded on activated carbon: kinetics and isotherm study. J Ind Eng Chem 20:17–28
Gupta VK (2009) Application of low-cost adsorbents for dye removal—a review. J Environ Manag 90:2313–2342
Gupta K, Khatri OP (2017) Reduced graphene oxide as an effective adsorbent for removal of malachite green dye: plausible adsorption pathways. J Colloid Interface Sci 501:11–21
Hameed BH (2009) Spent tea leaves: a new non-conventional and low-cost adsorbent for removal of basic dye from aqueous solutions. J Hazard Mater 161:753–759
Iranzad F, Gheibi M, Eftekhari M (2018) Synthesis and application of polythiophene-coated Fe_3O_4 nanoparticles for preconcentration of ultra-trace levels of cadmium in different real samples followed by electrothermal atomic absorption spectrometry. Int J Environ Anal Chem 98:16–30
Lee YC, Kim JY, Shin HJ (2013) Removal of Malachite Green (MG) from aqueous solutions by adsorption, precipitation, and alkaline fading using talc. Sep Sci Technol 48:1093–1101
Rajabi HR, Khani R, Shamsipur M, Vatanpour V (2013) High-performance pure and Fe^{3+}-ion doped ZnS quantum dots as green nanophotocatalysts for the removal of malachite green under UV-light irradiation. J Hazard Mater 250–251:370–378
Reife A, Reife A, Freeman HS (1996) Environmental chemistry of dyes and pigments. Wiley, Hoboken
Sadegh H, Shahryari-ghoshekandi R, Agarwal S, Tyagi I, Asif M, Gupta VK (2015) Microwave-assisted removal of malachite green by carboxylate functionalized multi-walled carbon nanotubes: kinetics and equilibrium study. J Mol Liq 206:151–158
Santhi T, Manonmani S, Smitha T (2010) Removal of malachite green from aqueous solution by activated carbon prepared from the epicarp of *Ricinus communis* by adsorption. J Hazard Mater 179:178–186
Sartape AS, Mandhare AM, Jadhav VV, Raut PD, Anuse MA, Kolekar SS (2017) Removal of malachite green dye from aqueous solution with adsorption technique using *Limonia acidissima* (wood apple) shell as low cost adsorbent. Arab J Chem 10:S3229–S3238
Srivastava S, Sinha R, Roy D (2004) Toxicological effects of malachite green. Aquat Toxicol 66:319–329
Wang D, Liu L, Jiang X, Yu J, Chen X (2015) Adsorption and removal of malachite green from aqueous solution using magnetic β-cyclodextrin-graphene oxide nanocomposites as adsorbents. Colloids Surf A Physicochem Eng Aspects 466:166–173
Xu R, Jia M, Zhang Y, Li F (2012) Sorption of malachite green on vinyl-modified mesoporous poly(acrylic acid)/SiO_2 composite nanofiber membranes. Microporous Mesoporous Mater 149:111–118
Yu F, Chen J, Yang M, Zhou L, Jin L, Su C, Li F, Chen L, Yuan Z, Yu L, Ma J (2012) A facile one-pot method for synthesis of low-cost magnetic carbon nanotubes and their applications for dye removal. New J Chem 36:1940–1943
Zhu Y, Murali S, Cai W, Li X, Suk JW, Potts JR, Ruoff RS (2010) Graphene and graphene oxide: synthesis, properties, and applications. Adv Mater 22:3906–3924